Thermal oxidation of poly(Dicyclopentadiene) – Decomposition of hydroperoxides

Huang Jing [1], Minne Wendy [2], Drozdzak Renata [2], Recher Gilles [2], Le Gac Pierre Yves [3], Richaud Emmanuel [1, *]

[1] Arts et Metiers Institute of Technology, CNRS, CNAM, PIMM, HESAM Université, F-75013, Paris, France
[2] TELENE SAS, 2 rue Marie Curie, 2 Rue Marie Curie, 59910, Bondues, France
[3] IFREMER, Service Matériaux et Structures, Centre de Brest BP70, 29280, Plouzané, France

* Corresponding author : Emmanuel Richaud, email address : emmanuel.richaud@ensam.eu

Abstract :

Thin unstabilized PDCPD film were thermally oxidized in ovens at several temperatures ranging from 50 °C to 120 °C. Hydroperoxide concentration was monitored by DSC. It was observed that hydroperoxides concentration reaches a plateau with short induction times, for example around 8 h at 50 °C. This plateau occurs at very high concentration, around about 1 mol l−1 at 50 °C. In order to study both the chemical mechanisms and the kinetics of hydroperoxides decomposition, oxidized samples were thermally aged in an inert atmosphere to destroy hydroperoxides. For initially high concentrations corresponding to the "plateau", it was shown that hydroperoxides decompose following a bimolecular process, the rate constant of which being calculated from the hydroperoxide depletion curves. The comparison of samples containing different polymerization catalyst amounts suggested the co-existence of an unimolecular process. This process mainly occurs at low hydroperoxides concentrations and slightly influences the overall oxidation process.

Highlights

► Quantification of peroxides in oxidized poly(dicyclopentadiene). ► Selective thermolysis experiments at low and high hydroperoxide concentration. ► Identification of uni- and bimolecular rate constants for POOH decomposition in PDCPD. ► Effect of polymerization catalysts on unimolecular rate constant.

Keywords : Polydicyclopentadiene, thermal oxidation, hydroperoxide decomposition, polymerization catalysts

1. INTRODUCTION

The polydicyclopentadiene (PDCPD) thermal oxidation was shown to induce an increase in T_g and yield stress, which was linked to a predominant crosslinking mechanism. The relative fastness of PDCPD oxidation compared to other unsaturated substrates (elastomers oxidized in their rubbery state) was first ascribed to the PDCPD glassy state involving a low termination rate between peroxy radicals [1], as evidenced from selective experiments under elevated oxygen pressures allowing the assessment of POO° + POO° termination rate constant [2].

Another possible reason to explain the high oxidation of thin PDCPD samples was the high initiation rate (i.e. rate of radical creation) [1,3]. In polymers below 150°C, there are several reasons to assume that the radical creation comes from defects found in (very) small concentration and from hydroperoxide decomposition. The latter becoming the main source of radicals creation at fast rates [4].

The rate constant for bimolecular POOH decomposition can in principle be determined from the modeling (fitting) of induction period length under oxygen excess whereas the unimolecular one could be estimated from the oxidation kinetics under lower oxygen pressure [5]. However, such method remains questionable since some other parameters (for example initial POOH concentration and propagation rate constants) must be somewhat arbitrarily fixed. In our last paper [2], we made the ad hoc assumption that oxidation was bimolecular (in term of radical creation by hydroperoxide decomposition) at least in the steady state but an unimolecular initiation reaction was also needed to fit the curves. The corresponding rate constants were only determined from curves "best fitting" and their values remain to us questionable. Last, we observed very high values of those initiation rate constants which were assumed to be linked with the presence of catalyst used for metathesis polymerization but the effect of these on the hydroperoxide decomposition remained to be better illustrated and quantified for us.

To investigate those questions linked to hydroperoxide decomposition, which is the aim of the present paper, we implemented here an alternative approach inspired from the analysis of signal related to peroxides or half time analysis [6,7,8] but using DSC instead of chemiluminescence, the advantage of DSC being more directly related to residual peroxides concentration [1]:

- selective thermolysis experiments with varying initial POOH concentration (being obtained from thermal oxidation experiments carried out at varying temperature and exposure times),

2

- comparisons of PDCPD with various residual amounts of organometallic Ring Opening Metathesis Polymerization catalysts (here Ruthenium based), since it is actually known that metallic ions (originating either from catalyst or sometimes fillers such clay) can be detrimental to the long term stability [9,10,11].

2. EXPERIMENTAL

2.1 Material

The samples under investigation were supplied as stabilized bulk material prepared by reaction injection molding process (RIM) at about 40°C. The catalyst used and the other information are summarized in Table 1. Films of 6-15 μm thickness were obtained by cutting the bulk material with a microtome (RM 2255 Leica), and then theses ones were purified by refluxing in CH_2Cl_2 (270997 Sigma-Aldrich) overnight. Unstabilized samples were stored in freezer (-20°C) for maximum 7 days before ageing.

Three materials were considered here. They were all synthesized using Ruthenium catalyst (Ru1 or Ru2), with low (L-PDCPD), medium (M*-PDCPD) and high (H-PDCPD) catalyst concentration. The structure of the Ru1 catalyst used for M*-PDCPD is given in Table 1. Ru2 catalyst used for synthesizing both L- and H-PDCPD differs from Ru1 by some substituent groups and is not given here because of confidentiality reasons.

According to the mechanism of Ring Opening Metathesis Polymerization, Ru based molecules are covalently bonded with polymer chains and would not be extractible during the purification process. It must be noted that ruthenium weight ratio is under the detection limits of elementary analysis and this last assumption could not be checked.
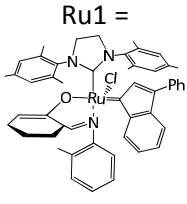
Material	Catalyst structure	Catalyst concentration (mol kg^{-1})	Antioxidant (in % mass fraction)	[C=C] (mol l^{-1})	[POOH]$_{t=0}$ (mol l^{-1})
M*-PDCPD	Ru1 =	2.52 10^{-4}	1%	13	0.001
L-PDCPD	Ru2	1.18 10^{-4}	/	11	0.024
H-PDCPD	Ru2	3.53 10^{-4}	/	11	0.013

Table 1. Details on materials under investigation. Initial concentration in hydroperoxides [POOH]$_{t=0}$ was measured by DSC. The double bonds concentration [C=C] was calculated from 733, 973 and 3049 cm^{-1} absorption [2]. NB: antioxidants, if any, were removed by CH_2Cl_2 extraction overnight.

2.2 Ageing and characterization

2.2.1 Ageing

Samples were aged at 50, 70, 90 and 120°C in ventilated ovens (supplied by System Climatic Service).

2.2.2 In situ hydroperoxides decomposition and quantification by differential scanning calorimetry (DSC)

Aged films were first analyzed using DSC in order to quantify peroxides by submitting aged samples to a heating ramp under nitrogen at a 10°C min^{-1} rate. The exotherm ascribed to POOH decomposition was converted into concentration using ΔH_{POOH} = 440 kJ mol^{-1} [1] by the formula:

[POOH] = ΔH / ΔH_{POOH} Eq. 1

Where ΔH is the measured enthalpy (in kJ kg^{-1}) and ΔH_0 the molar enthalpy for the hydroperoxide decomposition (kJ mol^{-1}) determined either from theoretical [12] assessment or correlation between DSC analysis and direct chemical chemical treatments (by iodometry for example [1,13]).

To better understand the stability of peroxides, the following procedure was used for samples thermally oxidized under air (with a concentration equal to [POOH]$_0$ after ageing) :

4

- heating to the ageing temperature under nitrogen at a 10°C min^{-1} rate

- isothermal under nitrogen at temperatures ranging from 50°C to 120°C (where hydroperoxides undergo decomposition)

- jump to 25°C and subsequent heating to 300°C under nitrogen by 10°C min^{-1} heating rate, this last step allows the titration of residual peroxides after thermolysis (expressed by [POOH]).
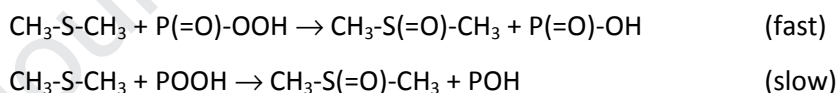
Analyses were done using a DSC Q10 apparatus (TA Instruments) with Aluminum pans and lids under 50 ml min^{-1} nitrogen flow. Results were analyzed using TA Analysis software.

2.2.3. Sulphur dioxide and Dimethyl sulfide chemical treatments

Sulphur dioxide (SO_2) treatments were used to verify the appearance of hydroperoxides, which transforms POOH into sulfates by the following reactions [14]:

$$POOH + SO_2 \rightarrow PO\text{-}SO_2\text{-}OH$$

$$PO\text{-}SO_2\text{-}OH + POOH \rightarrow POOP + H_2SO_4$$
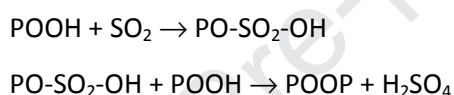
Dimethyl sulfide (DMS) treatments were also conducted to confirm the appearance of hydroperoxides [14]:

$$CH_3\text{-}S\text{-}CH_3 + P(=O)\text{-}OOH \rightarrow CH_3\text{-}S(=O)\text{-}CH_3 + P(=O)\text{-}OH \qquad \text{(fast)}$$

$$CH_3\text{-}S\text{-}CH_3 + POOH \rightarrow CH_3\text{-}S(=O)\text{-}CH_3 + POH \qquad \text{(slow)}$$

Degraded samples (5 mg) were placed in closed vessels and immersed :

- either in solutions of 5 mg of Na_2SO_3 (ref 71988 Sigma Aldrich) in 10 ml HCl (ref 40253 Sigma Aldrich, 37 wt % in H_2O) in which SO_2 was generated in situ,

- or in 10 ml DMS for 24 hours at room temperature.

2.2.4. Molecular changes observed by FTIR

Samples were characterized by Fourier Transform InfraRed spectroscopy using a Frontier apparatus (Perkin Elmer). Analyses were conducted in the 400 to 4000 cm^{-1} spectral range by averaging 4 scans at a 4 cm^{-1} resolution. Spectra were exploited using Spectrum software. In particular, we focused on the carbonyl absorbance (1850-1650 cm^{-1}) which was converted into concentration using Beer Lambert law with 300 l mol^{-1} cm^{-1} as molar absorptivity [1,2].

5

3. RESULTS

3.1 Hydroperoxides production in thermal oxidation

Titration of hydroperoxides in PDCPD by DSC was already presented in our previous papers [1,3]. An exothermic peak starting at about 80°C with a maximal heat release centered at 150°C (Figure 1, where thermograms are given for samples after various ageing times under air). This signal is totally removed by SO_2 (Figure 1a) or DMS treatment (Figure 1b). It shows that the species responsible for the exotherm monitored by DSC are hydroperoxides (associated or not [15,16]).

(a)   (b)
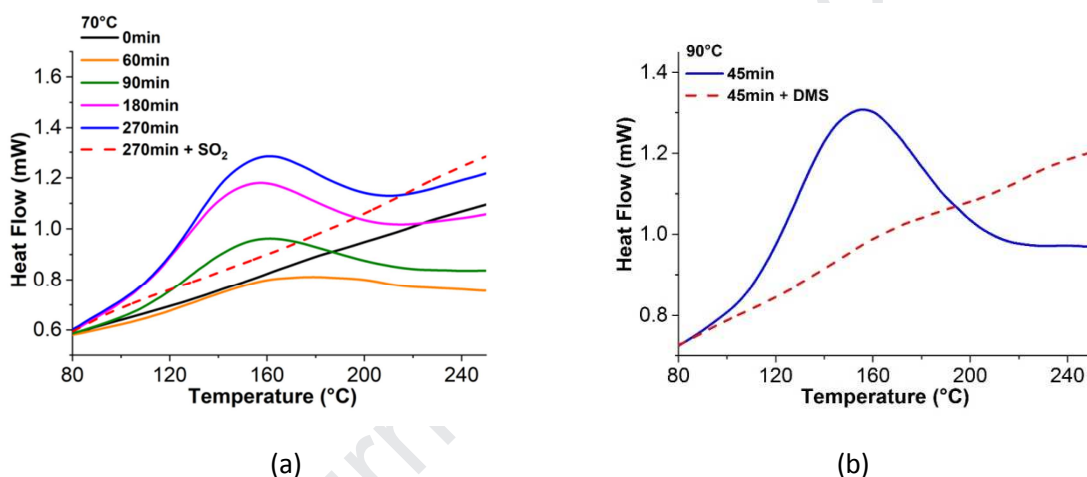
Figure 1. DSC thermograms of M*-PDCPD exposed at 70°C under air for various ageing times up to 270 min before (full line) and after (dashed line) SO_2 treatment (a), and exposed 45 min at 90°C under air before (full line) and after (dashed line) DMS treatment (b).

Using data from Figure 1, it is possible to measure the hydroperoxide concentrations during thermal oxidation of PDCPD. Results are plotted in Figure 2 for several ageing temperatures. For example, the POOH concentration at 50°C increases rapidly in the initial period to reach a value of about 1.5 mol l^{-1} after 10 h of exposure. A pseudo plateau was observed for each exposure conditions under investigation (50-120°C under atmospheric air).
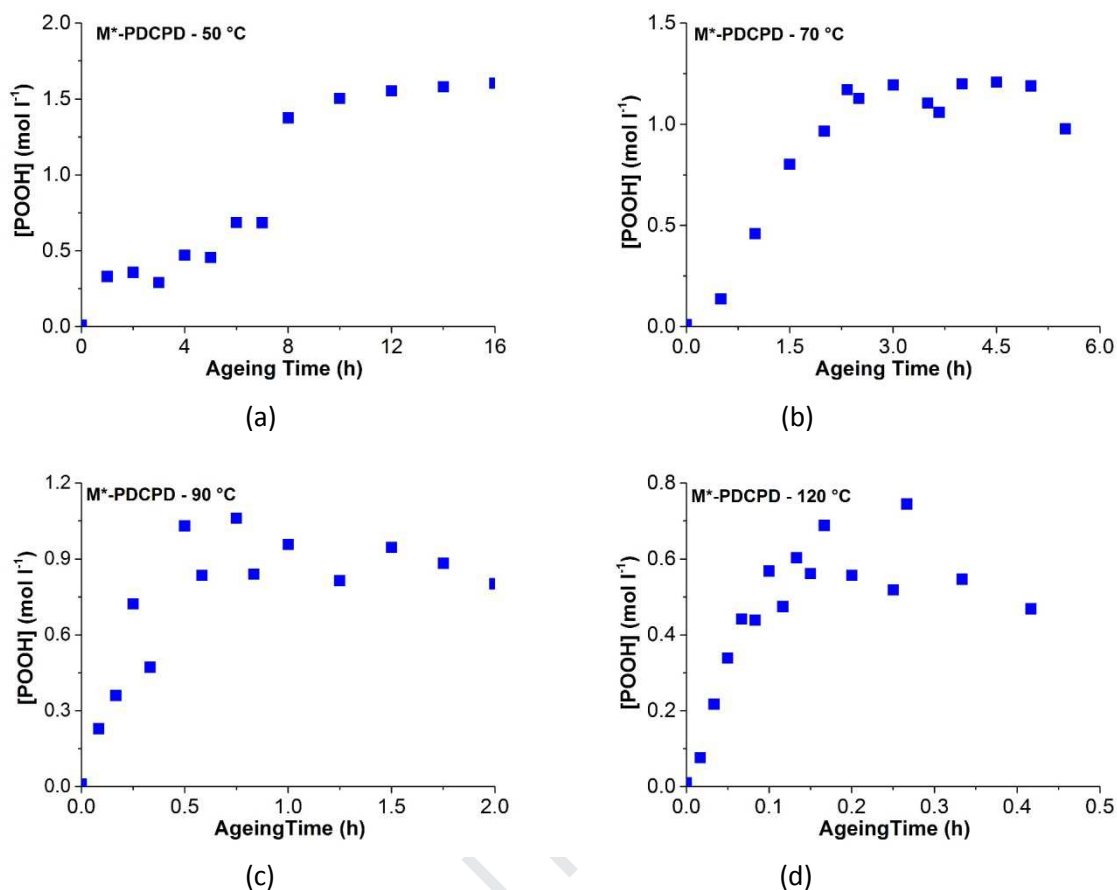
6

(a)

(b)

(c)

(d)

Figure 2. Changes in hydroperoxides concentration for thermal oxidation in PDCPD medium* at 50 (a), 70 (b), 90 (c) and 120°C (d).

3.2 Thermolysis of hydroperoxides

In order to investigate decomposition of hydroperoxides in PDCPD, thin samples were first oxidized under air (to reach a concentration denoted by $[POOH]_0$ as given in Figures 4, 8, 9 and 11). They were later in situ thermally aged using DSC under nitrogen atmosphere, after which residual hydroperoxides concentration was measured. Typical results are plotted in Figure 3.

7
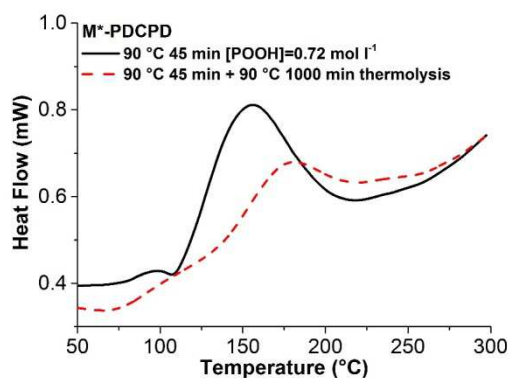
Figure 3. DSC thermograms before (full line) and after 1000 min thermolysis at 90°C (dashed line) for M*-PDCPD exposed 45 min at 90°C under air.

Two kinds of samples have been considered in this study:

- samples with a high concentration of hydoperoxides (i.e. when the plateau is reached)

- samples with a much lower hydroperoxide concentration (typically $[POOH]_0 \sim 0.1 - 0.3$ mol l^{-1}) so as to consider early state of the degradation.

Results for M*-PDCPD are presented in Figure 4.

8

(a)

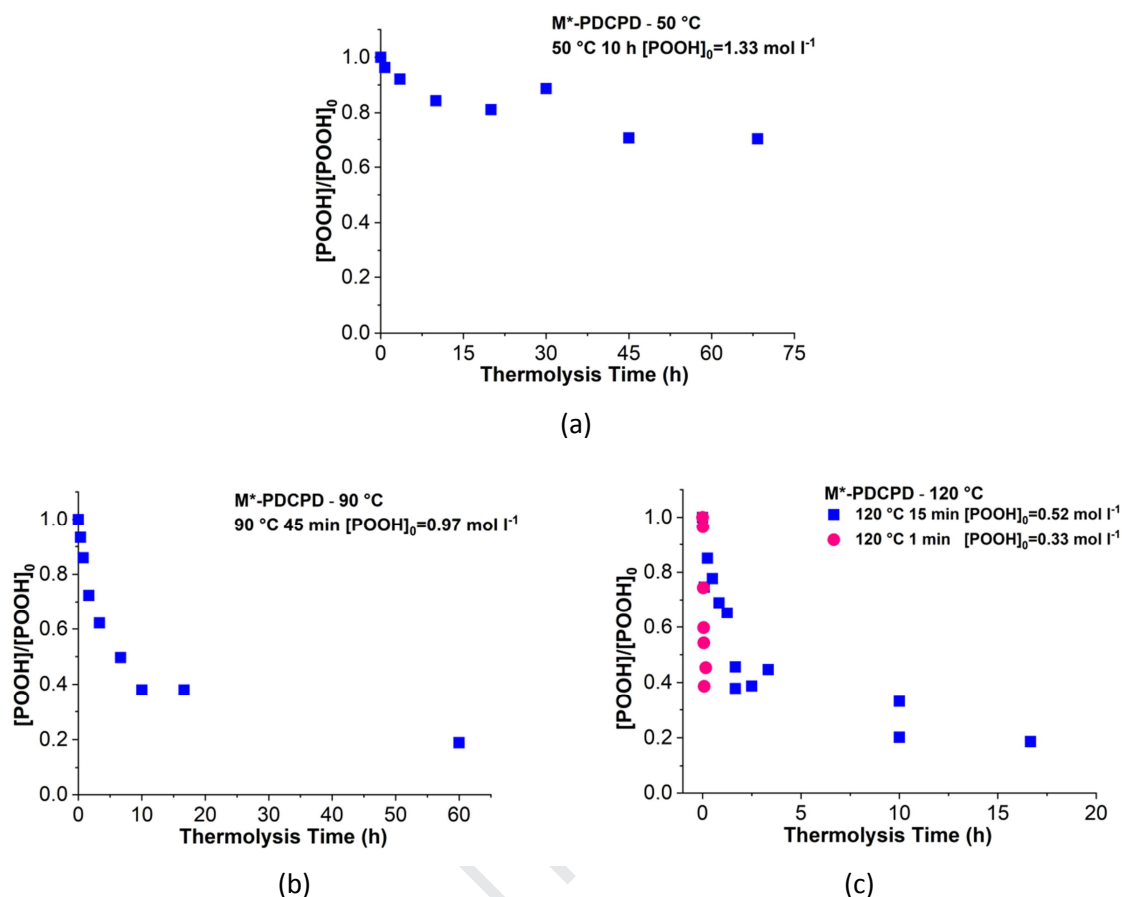(b)   (c)

Figure 4. Changes in normalized hydroperoxides concentration ($[POOH]_0$ is the hydroperoxide concentration after ageing under air – see Figure 2) for thermolysis of M*-PDCPD at 50 (a), 90 (b) and 120° C (c). NB: time to totally destroy POOH at 50°C was too long so that thermolysis were interrupted after 70 h.

The changes in residual concentration (normalized by the initial concentration after ageing under air i.e. at the beginning of thermolysis and expressed by $[POOH]_0$) versus thermolysis time are given in Figure 4. They display an auto-decelerated shape. The time to reach for example $[POOH]/[POOH]_0 = 0.5$ clearly decreases with temperature (about 2 h at 120°C, 7 h at 90°C, more than 100 h at 50°C).

Those sets of experiments were completed by investigating the kinetics of thermolysis in the "low concentration domain" (i.e. for samples oxidized during low exposure times: 1 min at 120°C under air, $[POOH]_0 = 0.33$ mol l^{-1}). In this case, the time needed for $[POOH]/[POOH]_0 = 0.5$ is only 4 minutes showing that the thermolysis mechanism is different in the "low concentration" and "high concentration" domains as it will be developed later.

The molecular changes observed by FTIR during those thermolysis experiments are shown in Figure 5. These results call for the following comments:

9

- Thermolysis always generates a decrease of hydroxyl band at 3400 cm^{-1}, and an increase of carbonyl band centered at 1710 cm^{-1} independent of temperature (Figure 5a). This suggests that there is no difference between carbonyl functions generated from alkoxyl radical (i.e. peroxide decomposition during either thermolysis or more generally thermal oxidation) in the investigated temperature range.

Using the difference in hydroperoxides concentration values Δ[POOH] (from DSC measurement) and the corresponding increase in carbonyl concentration Δ[P=O] (from FTIR), the apparent carbonyl yield from POOH decomposition (γ_1) can be obtained (Eq. 2):

$$\gamma_1 = \Delta[P=O]/\Delta[POOH] \qquad \text{Eq. 2}$$

γ_1 stays almost constant (ca 0.5) with temperature (Figure 5b). This value is higher than the value used for numerical simulation [2] or experimental data on polyisoprene [17]. γ_1 may be here overestimated because the thermolysis process also generates some peroxy radicals that can create other carbonyls for example from termination reactions (see Appendix 1).

(a)   (b)
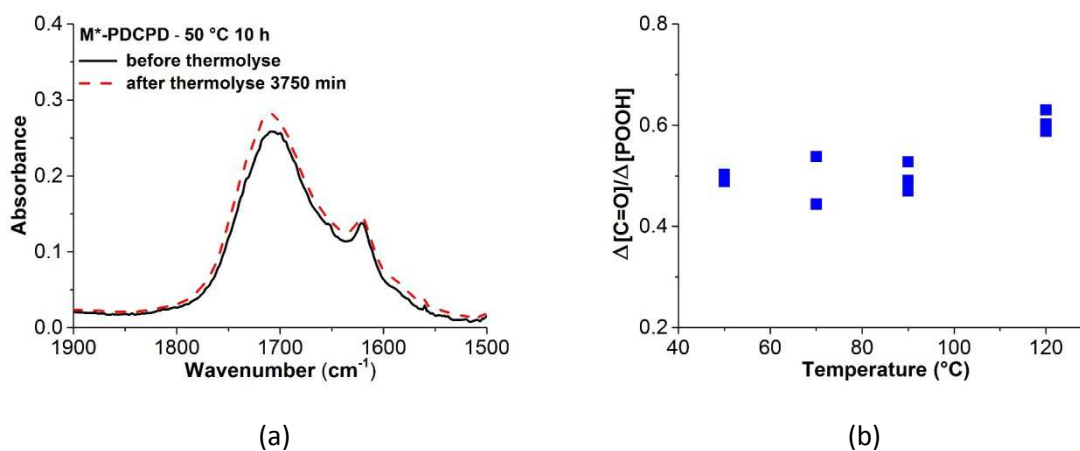
Figure 5. FTIR spectra for PDCPD before (full line) and after (dashed line) thermolysis at 50°C (a) and apparent carbonyl yield as a function of temperature (b).

3.3. Effect of catalyst

The oxidation kinetics of H-PDCPD and L-PDCPD catalysts PDCPD grades were compared (NB: PDCPD medium* was not studied here because it was not polymerized in the same conditions and does not display the same concentration in double bonds as the H-PDCPD and the L-PDCPD). It must be

10

specified that $[POOH]_{t=0}$ (before any ageing) was measured by DSC close to 0.024 mol l^{-1} for L-PDCPD and 0.013 mol l^{-1} for H-PDCPD.

Results are presented in Figure 6 for hydroperoxides and carbonyls concentrations. It shows that the presence of catalysts does not significantly change the overall kinetic curves for POOH whatever the temperature. As it will be seen later from Eq. 11 and 12, the small differences would rather come from experimental uncertainties than physical reasons associated to differences in catalyst concentration. In the meantime, results clearly show that the kinetics of carbonyl build-up are rather close for the two catalyst levels considered here. This is in particularly true for the induction period value and confirms the previous conclusion. A small but non negligible difference exists after the end of the induction period when the rate for carbonyl buildup is maximal. The latter will be discussed by kinetic modeling (Appendix 3). In other words, it seems that the presence of catalyst accelerates the polymerization process with only a minor detrimental effect on polymer stability.
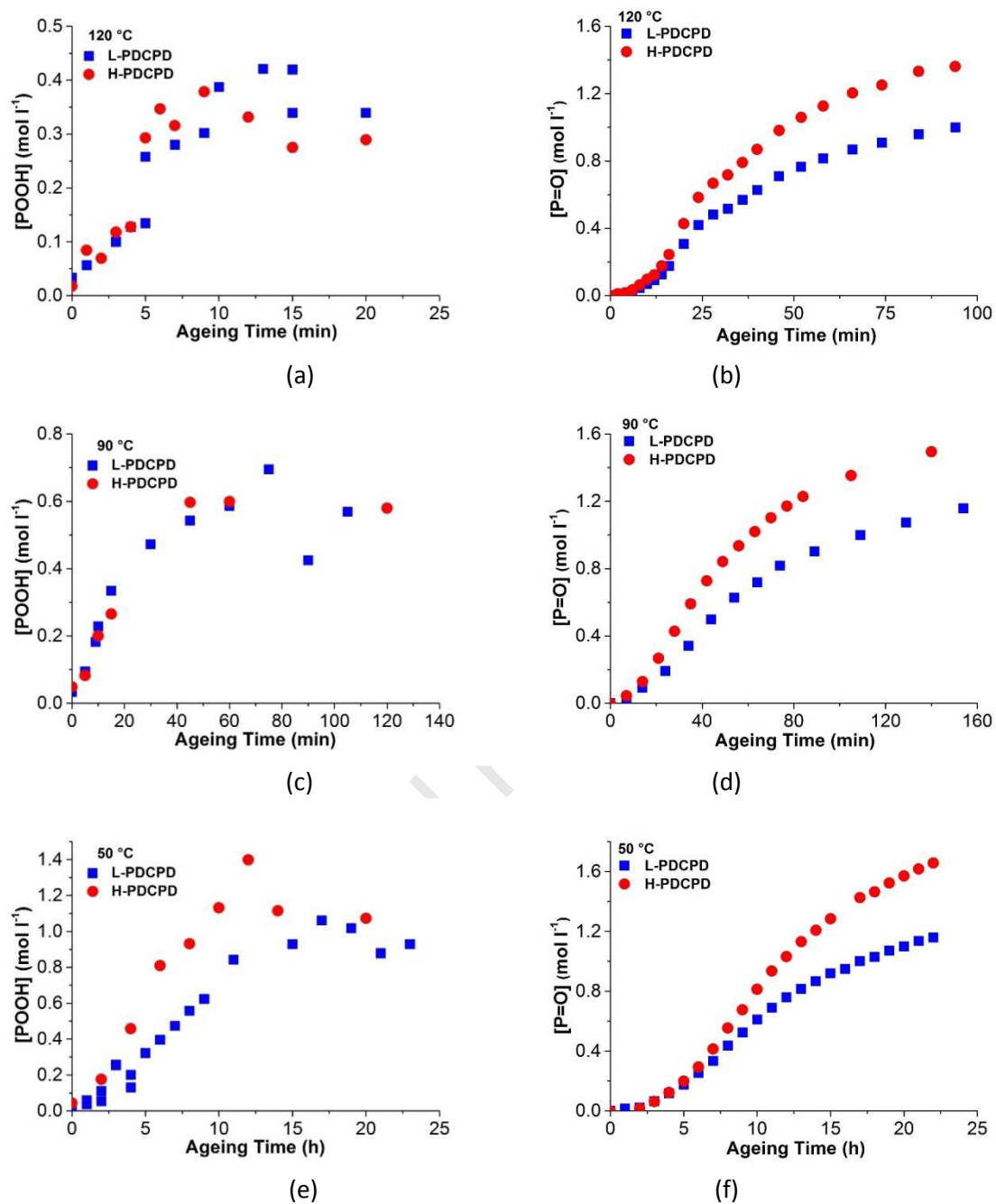
11

Figure 6. Changes in hydroperoxides and carbonyls concentrations for L-PDCPD samples (■), or H-PDCPD samples (●) catalyst content thermally oxidized at 120, 90 and 50°C under air.
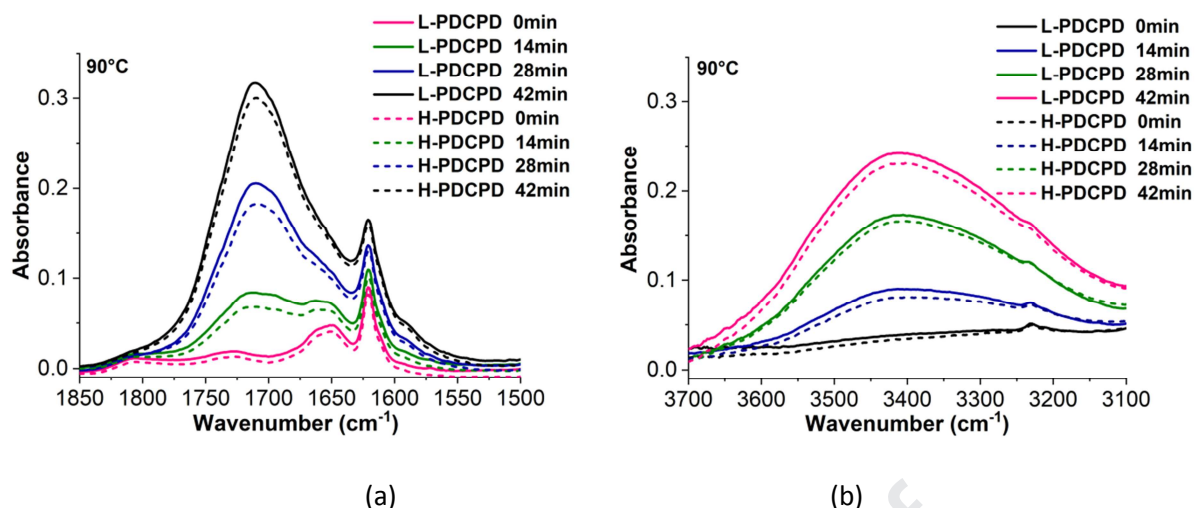
12

(a)   (b)

Figure 7. FTIR spectra of L-PDCPD (full line, 13.3 µm thickness) and H-PDCPD (dashed line, 12.8 µm thickness) exposed at 90°C under air.

The molecular changes of L-PDCPD and H-PDCPD with ageing time (Figure 7) display the classic features of thermal oxidation. An increase of hydroxyl band at ca 3400 cm^{-1} corresponds to oxidation products (e.g. hydroperoxides, alcohols or carboxylic acids) occurring in the thermal oxidation of other hydrocarbon polymers. Besides, an increase of carbonyl band centered at ca 1710 cm^{-1} is observed. Recalling the oxidation mechanisms of PDCPD explained in our last paper [2], the carbonyls mainly come from mechanisms detailed in Appendix 1.

① the initiation step by unimolecular and bimolecular decomposition of hydroperoxides.

② the bimolecular POO° termination involving the disproportionation of two alkoxy radicals [18,19]:

$$POO° + POO° \rightarrow P=O + POH$$
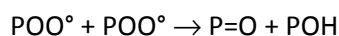
③ the decomposition of POOP° (coming from the addition reaction of POO° on double bonds), that rearrange into PO°.

Carbonyls formed from POOH decomposition are possibly aldehydes (and then carboxylic acids) whereas carbonyls formed from POO° are possibly ketones [1]. As it will be seen later, only the unimolecular decomposition is influenced by catalyst residue. The fact that the carbonyl absorbance seems the same in L-PDCPD and H-PDCPD (Figure 7a) seems to indicate that the contribution of unimolecular POOH decomposition is negligible in a first approach compared with the two other carbonyl sources.

13

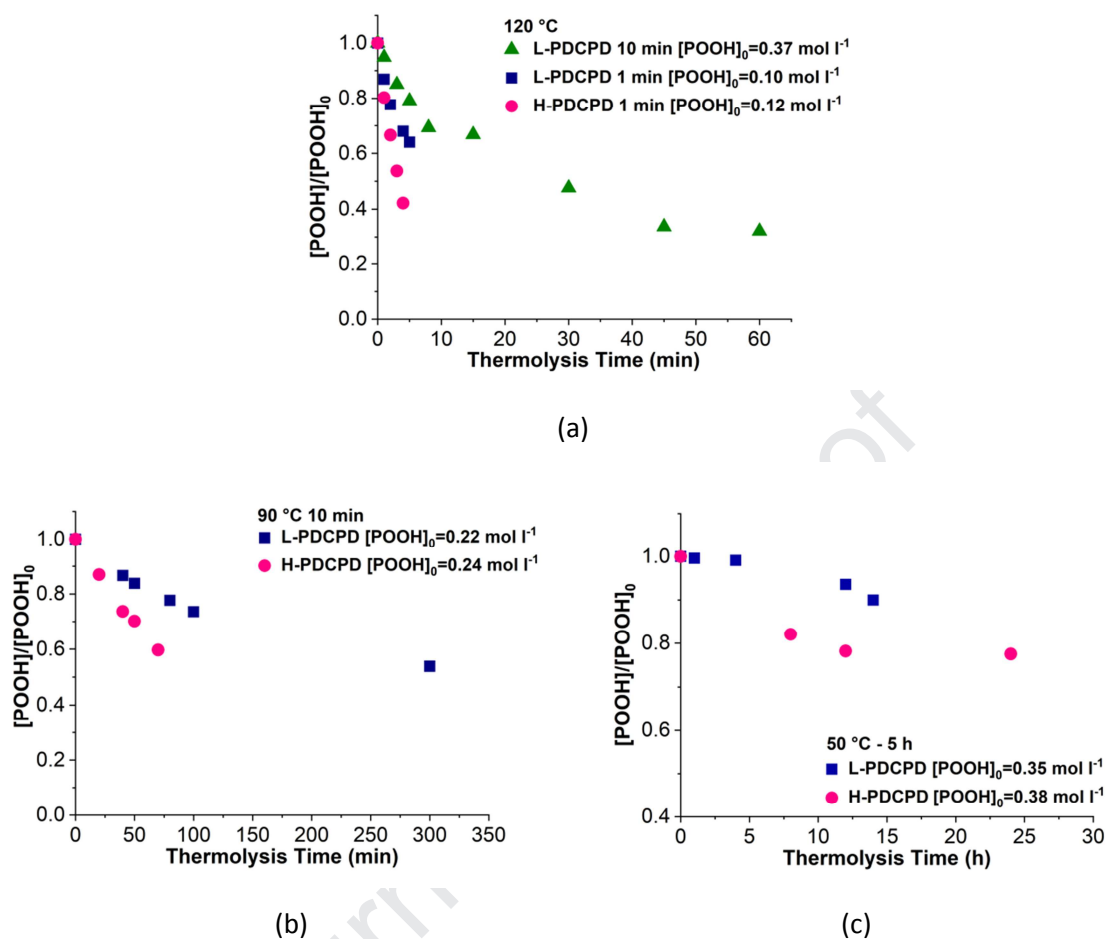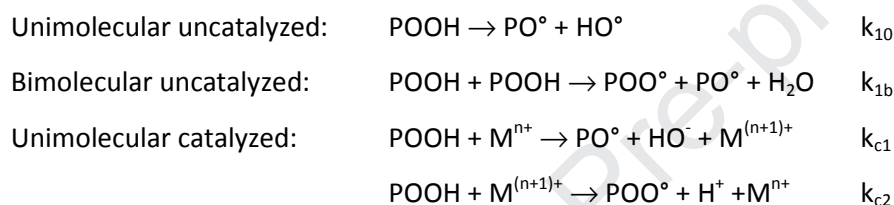Figure 8 shows the thermolysis results of L-PDCPD and H-PDCPD.

(a)

(b)

(c)

Figure 8. Changes in hydroperoxides concentration for thermolysis of L-PDCPD (▲ or ■) and H-PDCPD (●) at 120 (a), 90 (b) and 50°C (c). NB: the caption indicates the temperature and time for ageing under air, and the corresponding POOH concentration after ageing and before thermolysis – see Figure 6.

4. DISCUSSION

Our main aim is here to derive a set of rate constants for POOH decomposition from the thermolysis experiments reported in Figure 4. Such rate constants can in principle be used in kinetic models for radical oxidation [1,2] wit the advantage of being independently and more precisely assessed than by the mere best curves fitting of overall oxidation kinetics.

4.1. Theoretical investigation of the kinetics of POOH decomposition

Firstly, let us recall that, in the frame of this work, it seems that there are three modes (from a kinetic point of view) for POOH decomposition [20,21]:

Unimolecular uncatalyzed:	$POOH \rightarrow PO° + HO°$	k_{10}
Bimolecular uncatalyzed:	$POOH + POOH \rightarrow POO° + PO° + H_2O$	k_{1b}
Unimolecular catalyzed:	$POOH + M^{n+} \rightarrow PO° + HO^- + M^{(n+1)+}$	k_{c1}
	$POOH + M^{(n+1)+} \rightarrow POO° + H^+ + M^{n+}$	k_{c2}

The initiation step is composed of both uni- and bimolecular decomposition of POOH. The specific identification of both uni- and bimolecular rate constants is thus intricate (apart maybe in the case of oxidation under oxygen excess where bimolecular initiation predominates, but the identification of k_{1b} value remains somewhat dependent on the choice made for the other kinetic parameters in particular for propagation events).

It seems however that, depending on the level of hydroperoxide, reaction of radical creation from hydroperoxide decomposition are either predominantly uni- or bimolecular which makes it possible to selectively study each kind of initiation. Let us recall that:

$r_{uni} = -d[POOH]/dt = k_{10}[POOH]$ Eq. 3

$r_{uni\ catal} = -k_{1C}[M^+][POOH]$ Eq. 4

(k_{1C} depending both on k_{c1} and k_{c2} , and the concentration ruthenium catalysts in its several oxidations levels Ru^{2+}, Ru^{3+}, Ru^{4+} … which is not developed here).

In other words, the unimolecular process is possibly described by an apparent rate constant [22]:

15

$$k_{1u} = k_{10} + k_{1C}[M^+]$$
Eq. 5

If POOH decompose in an unimolecular process, their concentration would change according to the well know equation:

$$\ln[POOH] = -k_{1u}t + \ln[POOH]_0$$
Eq. 6

according to which the half-life time for the decay of hydroperoxides ($t_{1/2 \, uni}$) is given by:

$$t_{1/2 \, uni} = \ln 2 / k_{1u}$$
Eq. 7

If POOH decompose following a bimolecular process, the rate is given by:

$$r_{bi} = -\tfrac{1}{2}d(POOH)/dt = k_{1b}[POOH]^2$$
Eq. 8

$$\frac{1}{[POOH]} = 2k_{1b}t + \frac{1}{[POOH]_0}$$
Eq. 9

And the half-life time for the decay of hydroperoxides ($t_{1/2 \, bi}$) is given here by:

$$t_{1/2 \, bi} = 1/(2k_{1b}[POOH]_0)$$
Eq. 10

Let us note that in some cases, the situation is more complicated. For example, in PP, the decomposition takes place in two stages [23]. A fast decomposition is first observed, and is followed by a slow decomposition with a residual (persistent) concentration in POOH even at long thermolysis time. These two stages cannot be described by first- or second- order decay kinetics.

In our case, we considered separately thermolysis either at "plateau" (Figure 4) or at early stage (Figure 8). As results of experiments performed at 120°C show (Figure 4c), the mechanism (uni- or bimolecular) is not the same since time to divide initial by 2 is not the same for samples in the plateau and in the low concentration domain. To better distinguish if kinetics obey order 1 or order 2, residual hydroperoxide concentrations will be plotted in order 1 ($\ln [POOH]/[POOH]_0$ vs time) or order 2 ($1/[POOH] - 1/[POOH]_0$ vs time) diagrams and we will use the value of the regression coefficient (R^2) to decide which one of those two mechanisms was the most likely together with discussion of the physical validity of the proposed scenario.

16

4.2. On the decomposition of POOH at high concentration (pseudo plateau)

Despite some scatter, the regression correlation is higher for order 2 plots than order 1 (Figure 9). It seems thus that POOH decomposition obeys a second order kinetics i.e. POOH decompose in a bimolecular way. This is well in line with the FTIR observations showing the maxima of hydroxyl absorbance at 3400 cm^{-1} (Figure 7b).

A supplementary argument militating in favor of bimolecular process comes from the comparison of samples with various concentrations in catalysts residues. According to Figure 6, there is no significant effect of catalyst on the oxidation kinetics in particular on the maximal POOH concentration. As justified in Appendix 2, this latter is expressed in steady state (under oxygen excess):

- in unimolecular mode:

$$[POOH]_{max} = \frac{k_3^2 [PH]^2}{k_{1u} k_6}$$
Eq. 11

- in bimolecular mode:

$$[POOH]_{max} = \frac{k_3 [PH]}{2\sqrt{k_b k_6}}$$
Eq. 12

The maximal level of POOH for H-PDCPD and L-PDCPD catalyst concentration are the same so that:

- either $k_{1u\ high} = k_{1u\ low}$ which seems in contradiction with other results presented in the next paragraph (NB: the data at 50°C would even suggest $[POOH]_{high} > [POOH]_{low}$ meaning $k_{1u\ high} < k_{1u\ low}$, which in contradiction with any physical meaning).

- or $k_{1b\ high} = k_{1b\ low}$ which seems more likely since bimolecular process can be considered as an auto-assisted decomposition process which is not influenced by metallic catalyst concentration.
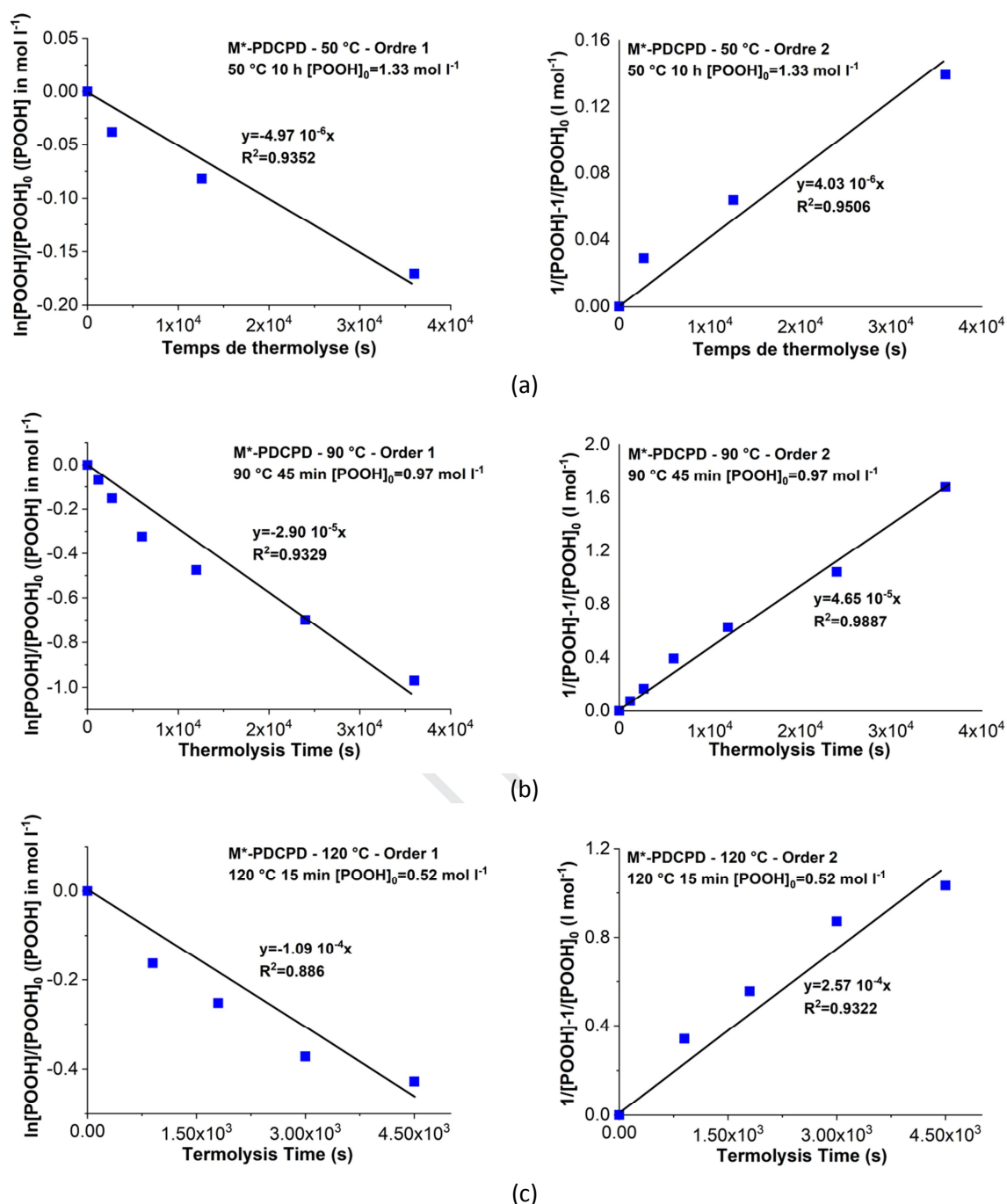
Figure 9. Linear equation of order 1 (left) and 2 (right) for M*-PDCPD thermolysis at pseudo plateau at 50 (a), 90 (b) and 120°C (c). NB: the caption indicates the time and temperature for ageing under air, and the corresponding POOH concentration after ageing and before thermolysis – see Figure 2).

Therefore k_{1b} values were determined by the half of the slope of second order diagrams (Figure 9). Interestingly, one sees that the observed values are well in line with $t_{1/2}$ values (Figure 4) and Eq. 8: for example at 120°C, $t_{1/2}$ is about 2 h which suggests $k_{1b} \sim 1.3 \times 10^{-4}$ l mol^{-1} s^{-1} which is in good agreement with slope value (Figure 9c). This validates for us the reasoning. Rate constants values

were then plotted in an Arrhenius diagram (Figure 10) together with other values from other substrates chosen because they contain C=C double bonds. Even if values between all polymers have the same order of magnitude in the investigated temperature range between PDCPD, Isoprene Rubber (IR) and Chloroprene Rubber (CR), their activation energy values differ (62 kJ mol^{-1} vs more than 100 kJ mol^{-1} for both elastomers). Values ranging from 70 to 120 kJ mol^{-1} are reported in the Denisov's monograph [20], with prefactor ranging from more than 10^2 to less than 10^{13} l mol^{-1} s^{-1} (vs about 2×10^4 here) and it remains to explain if the relatively low E_a value for PDCPD comes from experimental uncertainty or a physical effect facilitating the bimolecular process.
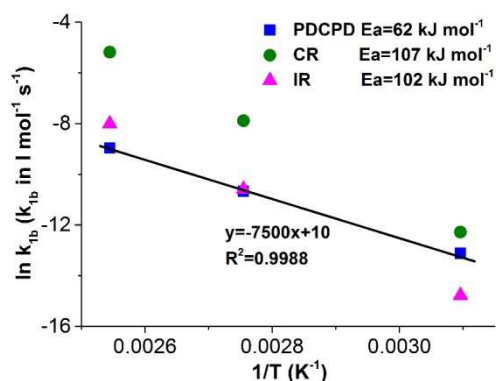

Figure 10. Arrhenius plot of k_{1b} values coming from thermolysis for PDCPD (■), CR (●) [24], IR (▲) [17] from best fitting of oxidation curves.

4.3. On the low hydroperoxide concentration domain (in early period)

The same theoretical treatment was applied for thermolysis experiments in the low concentration domain. Results are presented in Figure 11. In the domain of "low" POOH concentration (i.e. below 0.3 mol l^{-1}), POOH kinetics are clearly faster than those observed for initial POOH concentration (before thermolysis) at the plateau which can receive two interpretations: either the POOH involved in reactions are not the same, or they display a different reactivity (in terms of uni- or bimolecular process). Both hypotheses will be discussed here below.

Gijsman and al [23] showed similar peroxides decomposition rates with an initially fast decomposition ascribed to peracids whereas the slow decomposing ones would be hydroperoxides. In fact, the species responsible of DSC exotherm seem to react with SO$_2$ and DMS irrespectively of

19

the thermal oxidation time. In other words, it was difficult for us to identify each of those species and which one predominates depending on the conversion degree.
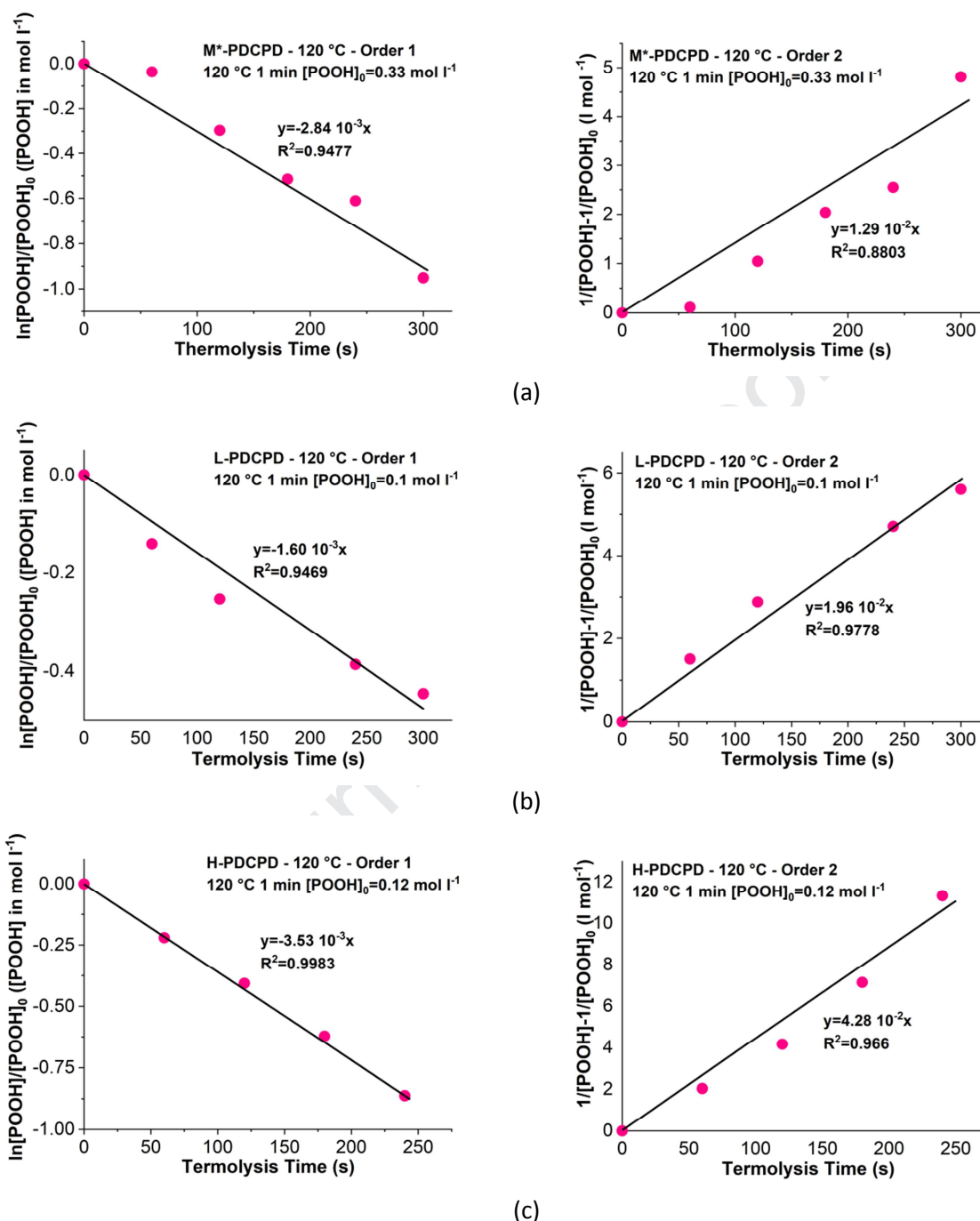

(a)

(b)

(c)

Figure 11. Kinetic order 1 and 2 of thermolysis for M*-PDCPD samples aged 1 min at 120°C (a); for L-PDCPD samples aged 1 min at 120°C (b); for H-PDCPD samples aged 1 min at 120°C (c). (NB: the caption indicates the ageing time and temperature under air, and the corresponding POOH concentration after ageing and before thermolysis – see Figures 2 and 6).

It seems however clear that the hypothesis of second order decomposition for low concentration is hard to support. The time to destroy half of initially present hydroperoxides in the case of thermolysis in early period is actually faster than the one of thermolysis in pseudo plateau. For example, $t_{1/2}$ for M*-PDCPD aged at 120°C for 15 minutes is 2 hours whereas $t_{1/2}$ for M*-PDCPD aged at 120°C for 1 minutes is 4 minutes. This agrees with the theoretical analysis ($t_{1/2\ uni}$ = ln 2/ k_{1u} and $t_{1/2\ bi}$ = ½k_{1b}[POOH]$_0$). The "unimolecular" mechanism was thus envisaged but, apart in some cases (high temperature and high catalysis content), the first order adjustment was not perfect. We thus envisaged the following scenario: in the "low concentration domain" investigated here, both decomposition modes are concomitant, i.e.:

$$d[POOH]/dt = - k_{1u}[POOH] - 2k_{1b}[POOH]^2 \qquad \text{Eq. 13}$$

with k_{1b} determined from the decomposition in the high concentration region (see previous paragraph). The values of k_{1u} were thus determined from the procedure illustrated in Figure 12, with a range of values [$k_{1u\ min}$ - $k_{1u\ max}$] aimed at taking into account the experimental uncertainties: for example at 90°C: k_{1u} would fall between 2.5 and 4.5 10^{-5} s^{-1}.
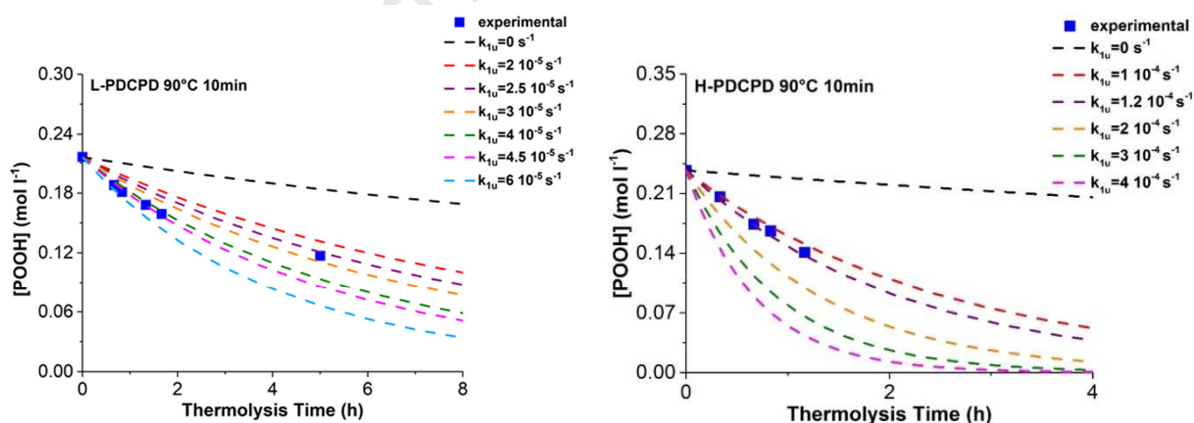

Figure 12. Numerical simulations for thermolysis of POOH (Eq. 13) with different value of k_{1u} at 90°C. NB: the dashed line with k_{1u} = 0 corresponds to the contribution of k_{1b} in thermolysis at initially low POOH concentration.

Then the k_{1u} values are plotted versus catalyst concentration and the ageing temperatures (Figure 13). The (apparent) rate constants identified from this procedure display two interesting characteristics:

- they increase with the catalyst content. Such a feature is typical of an unimolecular process. According to Eq. 3, a value for uncatalyzed unimolecular process (denoted by k_{10}) could be determined. The assumption of linear changes of k_{1u} with catalyst content is, however, for us an oversimplification since ruthenium can exist in several ionic forms (Ru^{2+}, Ru^{3+} and Ru^{4+} and Eq. 3 are a simplified description). The change of k_{1u} with the catalyst content could be described as $\ln[k_{1u}]$ varies linearly with the $\ln[catalyst]$ (Figure 13b). This characteristic leads to a new equation: $k_{1u} = k_{10} + k_{1C}[M^+]^x$ with $x = 0.65$ consistently with previous papers [25].

- they obey Arrhenius law (Figure 13b). If we consider separately data for L-PDCPD and H-PDCPD, prefactor (or frequency factor) range from $k_0 = 4 \times 10^{10}$ s^{-1} (H-PDCPD) to 48×10^{10} s^{-1} for L-PDCPD with $E_{1u} = 110$ kJ mol^{-1} (for L-PDCPD) to 100 kJ mol^{-1} (H-PDCPD). The activation energies display the expected order of magnitude for first order rate constants for hydroperoxide decomposition [15,20] (it seems possible however that catalyst presence induce a second order decrease). The prefactor values are lower than reported [17,26] and surprisingly k_{1u0} (L-PDCPD) > k_{1u0} (H-PDCPD), maybe due to the uncertainties of extrapolations in a Arrhenius diagram. It remains now to establish clear relationships between catalyst presence of prefactor and activation energies values.
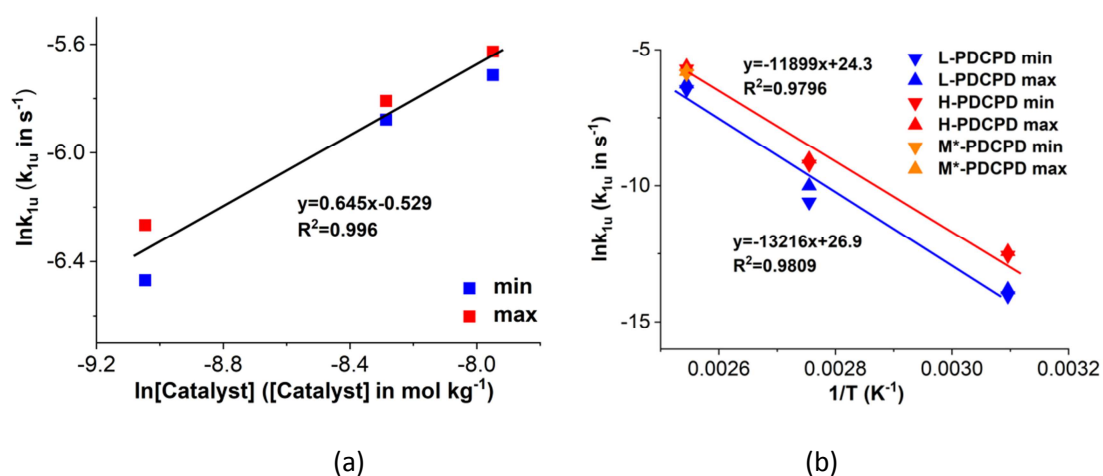

Figure 13. Change of k_{1u} with catalyst concentration at 120°C (a) and Arrhenius plot of k_{1u} for different PDCPD systemd (b). (NB: min and max values refer to the possible uncertainties associated to the determination method of k_{1u} and are given in Table 2).

Material	L, M, H-PDCPD	L-PDCPD	M*-PDCPD	H-PDCPD
Catalyst concentration (mol kg^{-1})		$1.18.10^{-4}$	$2.52.10^{-4}$	$3.53.10^{-4}$
Rate constants	k_{1b} (l mol^{-1} s^{-1})	k_{1u} (s^{-1})	
Estimation method	Treatment of experimental data (Fig. 9)	Simulation of thermolysis (Fig. 12)	Simulation of thermolysis	Simulation of thermolysis (Fig. 12)
T=50°C	2.02×10^{-6}	0.8×10^{-6} - 1.0×10^{-6}	/	3.5×10^{-6} - 4×10^{-6}
T=90°C	2.33×10^{-5}	2.5×10^{-5} - 4.5×10^{-5}	/	1×10^{-4} - 1.2×10^{-4}
T=120°C	1.29×10^{-4}	1.6×10^{-3} - 1.9×10^{-3}	2.8×10^{-3} - 3×10^{-3}	3.3×10^{-3} - 3.6×10^{-3}
E_a (kJ mol^{-1})	62	/	/	/
R^2	0.9999	/	/	/

Table 2. Summary of values of k_{1u} and k_{1b} measured by thermolysis experiments and by simulation.

NB: $k_{1u\ min}$ - $k_{1u\ max}$ express the possible values possible from estimation method in Figure 12.

k_{1u} and k_{1b} rate constants can in principle be used in the previously established kinetic model [2] with the advantage of being independently estimated. An example is given in Appendix 2. To complete it to get closer of real cases, some side reactions might still be taken into account in the modeling. For example, it seems possible that the metallic impurities progressively deactivate in contact with oxygen, water or any oxidation byproduct, inducing the decrease of the apparent unimolecular constant k_{1u} towards the uncatalyzed rate constant k_{1u0} (thus reducing even more the effect of catalyst on oxidation rate). Reversely, the possibility of POOH decomposition catalysis by oxidation products (alcohols, carboxylic acids) [27] occurring at high conversion degrees remains to be investigated. In any case, it seems that catalyst hardly influence the overall oxidation kinetics (Figure 6 and 7) which is very well described by kinetics model (Figure 14).

CONCLUSIONS

This paper present data related to the stability of hydroperoxides in PDCPD. Thermolysis experiments were performed to investigate the nature and kinetics aspects of the hydroperoxide decomposition reaction (uni- or bimolecular). Even if POOH seem to decompose mostly by bimolecular process, an unimolecular seems to be concomitant in the earlier exposure times, and would be favored by the use of high catalyst amount for the Ring Opening Metathesis Polymerization. The associated kinetics parameters were estimated and can be employed in a complete kinetic model for describing the whole oxidation process. The understanding of catalyst effect on thermal stability will be helpful to compound materials with the right tradeoff between fast polymerization and long term stability.
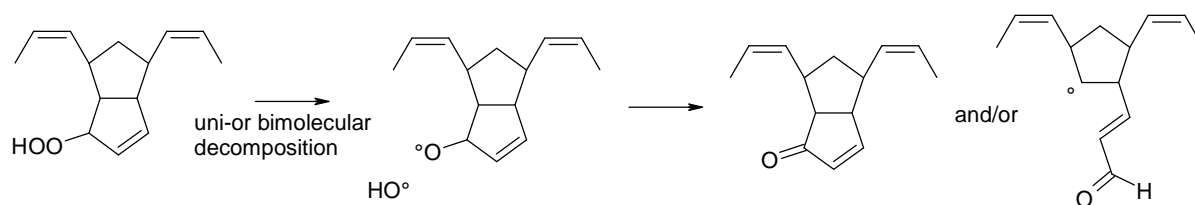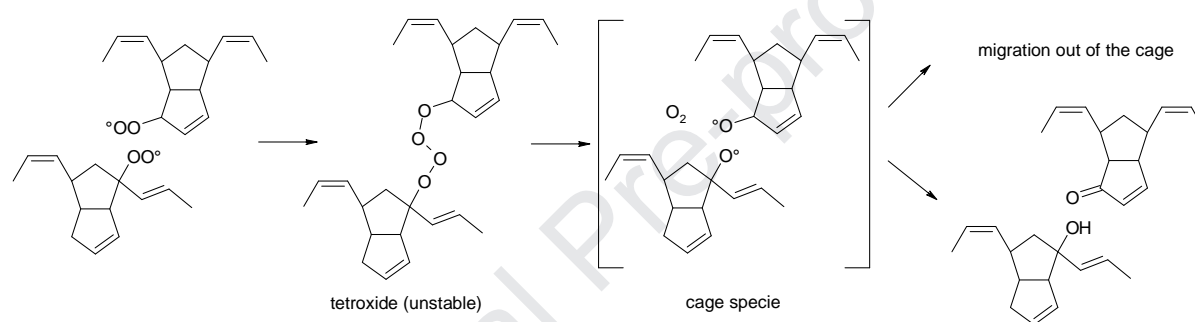
ACKNOWLEDGEMENTS

APPENDIX 1

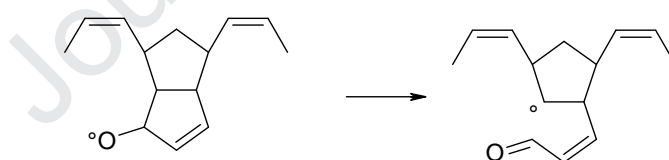The carbonyl functions can be produced from:

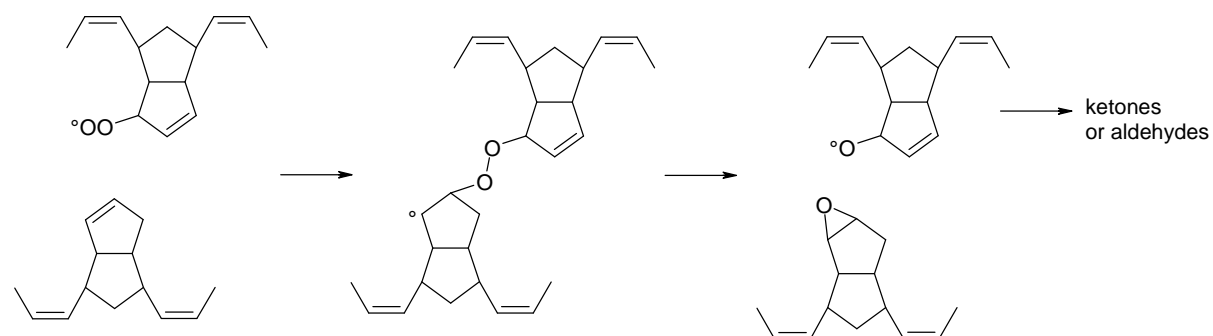① the initiation step of thermal oxidation: hydroperoxide decomposition

② the termination step involving several pathways [28]:

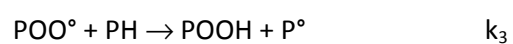Alkoxy radicals migrating out of the cage can decompose later by β-scission to give an aldehyde:

③ the propagation step by addition reaction of POO° to double bonds

25

APPENDIX 2

For demonstrating Eqs. 11 and 12, let us consider the simplified scheme for uni- and bimolecular reactions:

POOH $\rightarrow$ 2P° k_{1u}

P° + O_2 $\rightarrow$ POO° k_2

POO° + PH $\rightarrow$ POOH + P° k_3

POO° + POO° $\rightarrow$ inactive products k_6

NB: POOH actually decomposes into PO° and HO° but both radicals transform into alkyl so that unimolecular equation is here given in a kinetically equivalent equation [29].
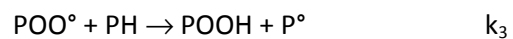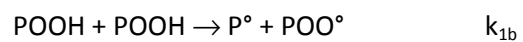
In steady state:

$\dfrac{d[POOH]}{dt} = 0$ $\Rightarrow k_{1u}[POOH] = k_3[POO°][PH]$

$\dfrac{d([P°]+[POO°])}{dt} = 0$ $\Rightarrow k_{1u}[POOH] = k_6[POO°]^2$

Which gives Eq. 11

In bimolecular case:

POOH + POOH $\rightarrow$ P° + POO° k_{1b}

P° + O_2 $\rightarrow$ POO° k_2

POO° + PH $\rightarrow$ POOH + P° k_3

POO° + POO° $\rightarrow$ inactive products k_6

In steady state:

$\frac{d[POOH]}{dt} = 0$ $\Rightarrow 2k_{1b}[POOH]^2 = k_3[POO°][PH]$

$\frac{d([P°]+[POO°])}{dt} = 0$ $\Rightarrow k_{1b}[POOH]^2 = k_6[POO°]^2$

Which gives Eq. 12

APPENDIX 3

From these modeling results in Figure 12, we got access to a range of k_{1u} values allowing the simulation of the thermal oxidation of L-PDCPD and H-PDCPD (Figure 14) and illustrating the model sensitivity to k_{1u}. It also suggests that for the longer time, initiation is mainly bimolecular but with a small proportion of unimolecular branching.
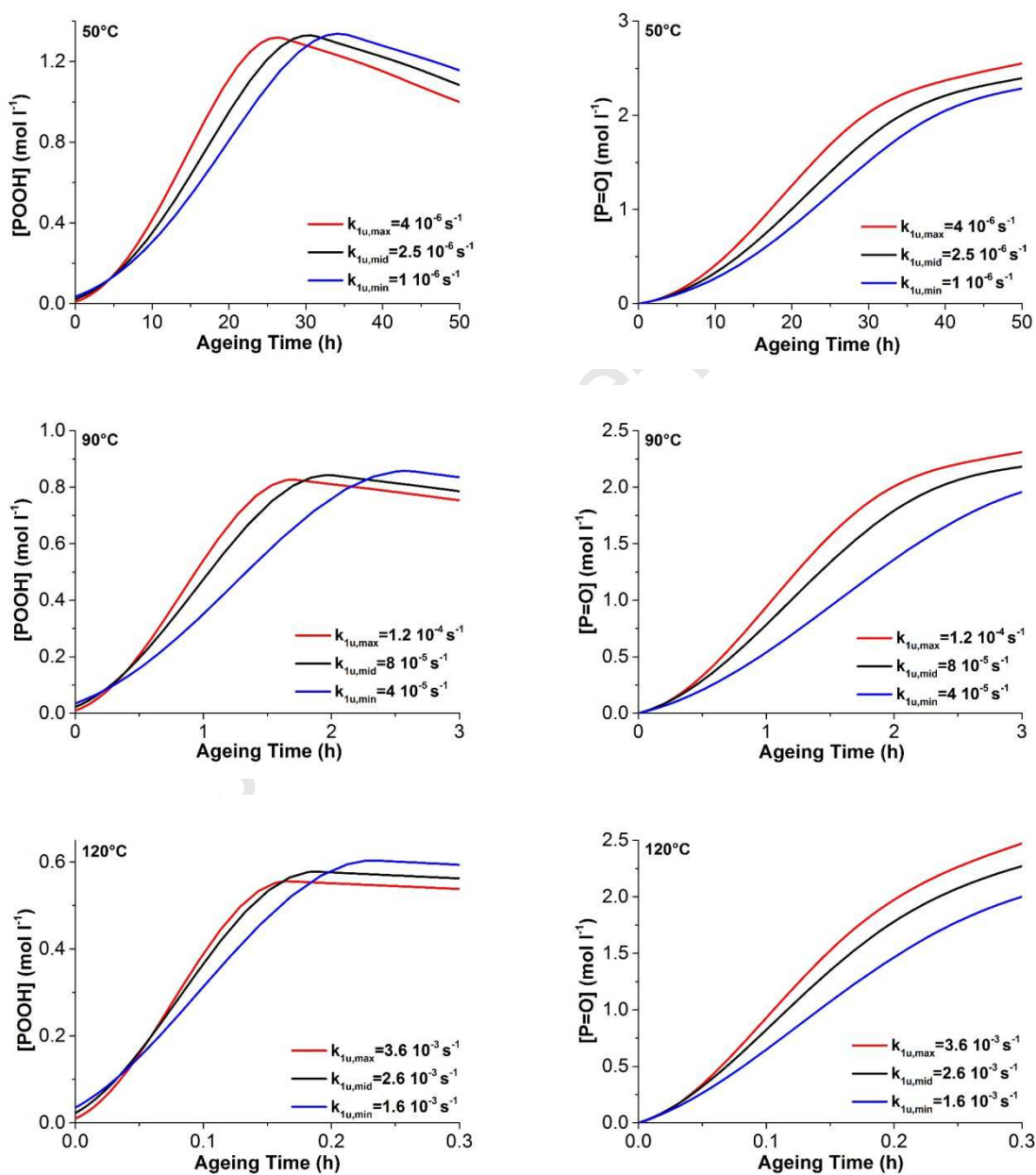

Figure 14. Numerical simulations for thermolysis of POOH with different value of k_{1u} (and $[POOH]_{t=0}$ values from Table 1).

28

REFERENCES

[1] E. Richaud, P.Y. Le Gac, J. Verdu. Thermooxidative aging of polydicyclopentadiene in glassy state. Polymer Degradation and Stability 102, 2014, 95-104.

[2] J. Huang, A. David, P.-Y. Le Gac, C. Lorthioir, C. Coelho, E. Richaud. Thermal oxidation of Poly(dicyclopentadiene)– kinetic modeling of double bond consumption. Polymer Degradation and Stability 166, 2019, 258-271.

[3] V. Defauchy P.-Y. Le Gac, A. Guinault, J. Verdu, G. Recher, R. Drozdzak, E. Richaud. Kinetic analysis of polydicyclopentadiene oxidation. Polymer Degradation and Stability 142, 2017, 169-177.

[4] L. Audouin, V. Gueguen, A. Tcharkhtchi, J. Verdu. "Close loop" mechanistic schemes for hydrocarbon polymer oxidation. Journal of Polymer Science Part A Polymer Chemistry 33, 1995, 921-927.

[5] E. Richaud, F. Farcas, P. Bartoloméo, B. Fayolle, L. Audouin, J. Verdu. Effect of oxygen pressure on the oxidation kinetics of unstabilised polypropylene. Polymer Degradation and Stability 91, 2006, 398–405.

[6] N.C. Billingham, M.N. Grigg. The kinetic order of decomposition of polymer hydroperoxides assessed by chemiluminescence. Polymer Degradation and Stabilty 83, 2004, 441-451.

[7] N.C. Billingham, E.T.H. Then, A. Kron. Chemiluminescence from peroxides in polypropylene: II. Luminescence and kinetics of peroxide decomposition. Polymer Degradation and Stability 55, 1997, 339-346.

[8] L. Zlatkevich. On the kinetic order of decomposition of polymeric hydroperoxides. Polymer Degradation and Stability 83, 2004, 369-371.

[9] G. Gutiérrez, F. Fayolle, G. Régnier, J. Medina. Thermal oxidation of clay-nanoreinforced polypropylene. Polymer Degradation and Stability 95, 2010, 1708-1715.

[10] E.M. Hoàng, N.S. Allen, C.M. Liauw, E. Fontán, P. Lafuente. The thermo-oxidative degradation of metallocene polyethylenes. Part 1: long-term thermal oxidation in the solid state. Polymer Degradation and Stability 91, 2006, 1356-1362.

[11] E.M. Hoàng, N.S. Allen, C.M. Liauw, E. Fontán, P. Lafuente. The thermo-oxidative degradation of metallocene polyethylenes: Part 2: Thermal oxidation in the melt state. Polymer Degradation and Stability 91, 2006, 1363–1372.

[12] Y. Ouldmetidji, L. Gonon, S. Commereuc, V. Verney. A differential scanning calorimetry method to study polymer photoperoxidation. Polymer Testing 20, 2001, 765-768.

[13] E. Richaud, F. Farcas, B. Fayolle, L. Audouin, J. Verdu. Hydroperoxide titration by DSC in thermally oxidized polypropylene. Polymer Testing 25, 2006, 829-838.

[14] D.J. Carlsson, R. Brousseau, D.M. Wiles, Reactions of sulfur dioxide with oxidized polyolefins. Polymer Degradation and Stability 15, 1986, 67-79.

[15] J.C.W. Chien, E.J. Vandenberg, H. Jabloner. Polymer reactions. III. Structure of polypropylene hydroperoxide. Journal of Polymer Science A1 6, 1968, 381-392.

[16] J.C.W. Chien, H. Jabloner. Polymer reactions. IV. Thermal decomposition of polypropylene hydroperoxides. Journal of Polymer Science A1 6, 1968, 393-402.

[17] X. Colin, L. Audouin, J. Verdu. Kinetic modelling of the thermal oxidation of polyisoprene elastomers. Part 1: Unvulcanized unstabilized polyisoprene. Polymer Degradation and Stability 92, 2007, 886–897.

[18] G.A. Russell. Deuterium-isotope Effects in the Autoxidation of Aralkyl Hydrocarbons. Mechanism of the Interaction of Peroxy Radicals. Journal of American Chemical Society 79, 1957, 3871-3877.

[19] G.A. Russell. The Rates of Oxidation of Aralkyl Hydrocarbons. Polar Effects in Free Radical Reactions. Journal of American Chemical Society 78, 1956, 1047-1054.

[20] E. Denisov, I. Afanas'ev, Oxidation and Antioxidants in Organic Chemistry and Biology, CRC Press, 2005. Chap 4. p .154.

[21] F. Gugumus. Physico-chemical aspects of polyethylene processing in an open mixer6. Discussion of hydroperoxide formation and decomposition. Polymer Degradation and Stability 68, 2000, 337-352.

[22] E.A. Moelwyn-Hughes. The Kinetics of Reaction in Solutions. Oxford University Press, London (1947), p. 297.

[23] P. Gijsman, J. Hennekens, J. Vincent. The mechanism of the low-temperature oxidation of polypropylene, Polymer Degradation and Stability 42, 1993, 95-105.

[24] P.Y. Le Gac, G. Roux, J. Verdu, P. Davies, B. Fayolle, Oxidation of unvulcanized, unstabilized polychloroprene: A kinetic study. Polymer Degradation and Stability 109, 2014, 175-183.

[25] W.H. Richardson. Metal Ion Decomposition of Hydroperoxides. IV. Kinetics and Products of Copper Salt Catalyzed Decomposition of t-Butyl Hydroperoxide. Journal of the American Chemical Society 88, 1966, 975-979.

[26] E. Denisov, I. Afanas'ev, Oxidation and Antioxidants in Organic Chemistry and Biology, CRC Press, 2005. Chap 4. Table 4.11.

[27] E. Denisov, I. Afanas'ev, Oxidation and Antioxidants in Organic Chemistry and Biology, CRC Press, 2005. Chap 4. p. 164.

[28] R. Lee, G. Gryn'Ov, K.U. Ingold, M.L. Coote. Why are: Sec -alkylperoxyl bimolecular self-reactions orders of magnitude faster than the analogous reactions of tert -alkylperoxyls? the unanticipated role of CH hydrogen bond donation. Physical Chemistry Chemical Physics 18, 2016, 23673-23679.

[29] L. Audouin, V. Gueguen, A. Tcharkhtchi, J. Verdu. "Close loop" mechanistic schemes for hydrocarbon polymer oxidation. Journal of Polymer Science Part A Polymer Chemistry 33, 1995, 921-927